VOL. 11, NO. 10, MAY 2016 ISSN 1819-6608
ARPN Journal of Engineering and Applied Sciences

www.arpnjournals.com

INVESTIGATION OF FILM COOLING EFFECTIVENESS FROM CYLINDRICAL COOLING HOLE WITH ANTI VORTEX GENERATOR BY NUMERICAL SIMULATION

A. A. Abu Zarida[1] and H. B. Salih[2]
[1]Faculty of Mechanical and Manufacturing Engineering, University Tun Hussein Onn Malaysia, Parit Raja, Johor, Malaysia
[2] Department of Plant and Automotive Engineering, University Tun Hussein Onn, Malaysia
E-Mail: abdoabuzrida@yahoo.com

ABSTRACT

This study deals numerical study of the effect of anti-vortex generator (AVG) on the film cooling performance of a circular cooling hole which has diameter (d = 20 mm) on a flat plate. The interaction between the jet cooling air and mainstream will result kidney vortex which will eliminate the film cooling effectiveness. Two types of AVG with different heights (H = 0.5 d and 0.25 d) are designed to eliminate the kidney vortex and investigate best film cooling effectiveness, where each of them is mounted to the flat plate upstream of the cooling hole by changing its lateral positions (A = 0.0 d, 0.25 d, 0.5 d and 0.75 d) with respect to the hole centerline and for each type has different distance respect to hole centerline. The changing of blowing ratio (BR = 0.5-1.0) was considered in this study. Simulation model has been used to simulate a film cooling configuration by using shear stress transport (SST) model. The results have been presented in terms of laterally averaged and maximum value of film cooling comparison graphs, velocity field on x/d = 3.0, vorticity on x/d = 3.0 and film cooling distribution which explained how the results obtained. Cases 04 and 07 gave the best positions for AVG where case 04 gave wide covered for laterally average film cooling effectiveness (η = 0.35), while case 07 gave the highest expand distribution and the maximum value for film cooling effectiveness (η = 0.66).

Keywords: film cooling effectiveness, blowing ratio, counter rotating vortex pair.

INTRODUCTION

Increasing demand for better performance of gas turbine requires rising in turbine inlet temperature. Nowadays, the gas turbines work at the temperature range around 1800K- 2000K, what is much higher than the melting temperature of the turbine components materials. Such increasing of the turbine inlet temperature became possible because of application of cooling scheme on the turbine components. Film cooling is the injection of cold air to provide a layer of cool fluid between the hot gases and the blade surface, reducing heat transfer to the surface.

Counter-rotating vortex pair (CRVP) promotes lift-off of cooling air. Then, the technique for controlling CRVP has been studied since long time ago. The geometry of the cooling hole exit is known as one of the most important factor which affects the film cooling performance and vortex structures (Haven *et al.* 1997). As another concept for the controlling (CRVP), some techniques have been used in which surrounded of a cooling hole as using ramp placed at the upstream of the film cooling holes (Na and Shih, 2007), (Barigozzi, Franchini and Perdichizzi, 2007),

A significant improvement can be achieved in the cooling performance of the film by the use different kinds of exit holes shapes. Investigation the effect of the expansion angle of the diffuser, the inclination angle of the hole, and the length of the cylindrical part at the entrance of fan shaped and cylindrical holes (Saumweber and Schulz, 2008). Morever, the compound-angle holes, either shaped or not, shows a better film cooling effectiveness than simple angle holes, but increase the heat transfer coefficient. Shaping will helps to maintain the cooling jets closer to the surface and will reduces the mixing effect as well as improves the coverage of film cooling in general (Azzi and Jubran, 2006). Another technique was used to reduce the lift-off of cooling air which is by using a 10 deg spanwise-diffused hole and found that the shaped hole provided better film cooling characteristics than commonly used cylindrical holes. As a result, the coolant had less penetration into the mainstream when compared to the cylindrical holes, and the film cooling performance was enhanced (Goldstein, Eckertand and Burggraf, 1974).

Many researchers proposed other methods such as changing of blowing ratio in order to investigate better film cooling effectiveness along the blades surface. The blowing ratios (BR) strongly affect the result. The film cooling effectiveness has increased along with the increase of blowing ratio. However, when the blowing ratio exceed beyond an optimum value, the effectiveness will be reduced (Christian *et al.* 2012)

Some of researches concentrated about the effect of inclination angle to the film cooling. If the angle between hole axis and the surface more steeper, there will be more coolant mixes with the hot gas, which means there will be no contribution to the cooling of the surface (Christian *et al.* 2012). The changing of cylindrical hole inclination angle of 30 °, 60 ° and 90 ° in a flat plate with a blowing ratio ranges from 0.33 to 2, and constant hole length in all cases. It observed that 30 ° had the best film cooling effectiveness with different blowing ratio (Yuen and Martinez, 2003).

This study deals numerical study of the effect of anti-vortex generator (AVG) on flat plate film cooling. This study relies on (Kawabata *et al.* 2014) in terms of the computational domain, geometry of (AVG) and the boundary condition. The difference between present study and (Kawabata *et al.* 2014) study was only the changing of (AVG) design. Where the first design based on Kawabata *et al.* 2014) method while the second design based on porposed method. In this investigation, film cooling effectiveness, the flow field, and the temperature field were revealed by using CFD approach.

METHODOLOGY

Geometry

The geometry will be corresponding to the experiment geometry (Kawabata *et al.* 2014). In the experiment, the main stream goes over the flat plate with a row of 4 cylindrical cooling holes, which are 35 degree inclined against the plate. The hole length to diameter ratio is l/d ≅ 3.5. The cooling holes are fed with air from a plenum. The cooling holes have a diameter (d) of 20 mm. The hole pitch, p, was 60 mm (3d). The upstream distance (10d) from the leading edge of the cooling hole and downstream distance (20d) behind the leading edge of the hole. The height above the flat plate is (6d) and the rest of dimensions shown in figure-1.

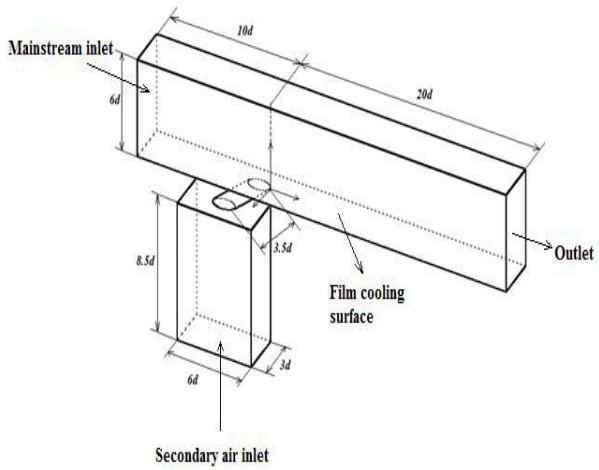

Figure-1. Computational domain.

Geometry of AVG

The geometry of film cooling hole and anti vortex generator (AVG) had several attempts were made to control the cooling air from the cooling hole by AVG proposed in this study. The employed AVG had elliptic base and front shapes with fillet at the root section. In this research, there are two groups of cases (AVG position). The first group, The streamwise distance from the center of a cooling hole to AVG, the length of the z axis orientations of AVG, the length of the x axis orientations of AVG, and the radius of a fillet were 1.5d, 1.0d, 0.5d, and 0.15d, respectively. As shown in figure 2. The height of AVG (H), and the off-set distance (literally position distance) of AVG from the center of a cooling hole (A) are listed in Table-1.

Table-1. AVG parameters for the first group.

Case	H	A
Basic	No AVG	No AVG
Case 01	0.5 d	0.0 d
Case 02	0.5 d	0.25 d
Case 03	0.5 d	0.5 d
Case 04	0.5 d	0.75 d

In the second group, the different only for the stream wise distance which was 1.5d to become 2d and the height of AVG (H) which was 0.5d to become 0.25 d. The parameters for second group are listed in Table-2.

Table-2. AVG parameters for the second group.

Case	H	A
Case 05	0.25 d	0.0 d
Case 06	0.25 d	0.25 d
Case 07	0.25 d	0.5 d
Case 08	0.25 d	0.75 d

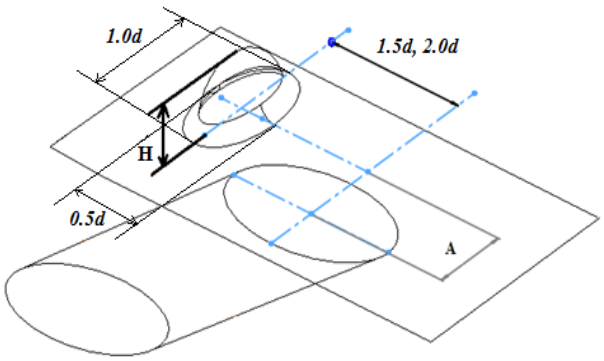

Figure-2. The geometry of anti-vortex generator (AVG).

Computational grid

The grid has been carried out hybrid type which is definitely (Tetrahedrous mesh) in this research as shown in Figure-3. That means contains the structured and unstructured mesh. The body has built unstructured, but the structured mesh has inflation from film cooling surface (wall surface) because it uses in order to resolve boundary layer at near film cooling surface. The number of nodes and elements which used to simulate the air flow are 243389 and 981839 respectively.

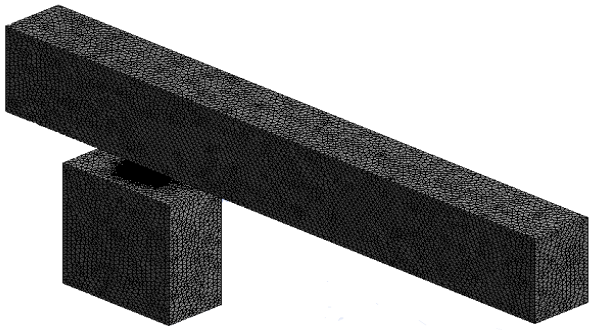

Figure-3. Isometric view of the meshing model for all geometry cases using CFX.

Boundary conditions

All tests were based on (Kawabata *et al.* 2014) in the wind tunnel at Reynolds number of 16400 based on film cooling hole diameter (d).

Table-3 shows the parameters that given from experimental data.

Table-3. Boundary conditions parameters.

Fluid model	Turbulence model	SST
Coolant Reynolds number	Re	16,400
Mainstream velocity	U_∞	13m/s
Mainstream temperature	T_∞	300 K
Coolant temperature	T_c	353 K
Blowing ratios	BR	0.5-1.0
Mainstream turbulence intensity	Ω_u	1%
Coolant jet turbulence intensity	Ω_c	1%
Density ratio	DR	0.85
Pressure	P	0 Pa

Secondary air velocity can be calculated from blowing ratio (BR) formula as follow.

$$(BR = \rho_c U_c / \rho_\infty U_\infty) \quad (1)$$

ρ_c = Cool air density
ρ_∞ = Mainstream density
U_∞ = Mainstream velocity
U_c = Cool air velocity

RESULTS

Velocity fields

Figure-4 shows the dimensionless u-velocity contours plots on the YZ plane (normal plane) at x/d=03 obtained by CFD simulation. As shown in the figures were vector plots of *v* and *w* components. A low velocity region (A) was observed by z/d = 0.0 in BR = 0.5 and this velocity incresed gradually when the secondary air velocity increased which means at higher BR = 1.0. This is a region where the mainstream and secondary air were mixing each other. The lift-off of secondary air was promoted in case 01 and case 02 for BR = 0.5-1.0, the low velocity region was located at higher position than basic case. In case 03 and case 04, u-velocity was decreased by the vortex generated from AVG (see figure 4 (a)). In case 05, case 06, case 07 and case 08, u-velocity was a little bit decresed comparing with case 04. The four recent cases have shown that there is no large change in u-velocity and low velocity region was usually similar as well.

Counter rotating vortex pair (CRVP)

Mostly, the (CRVP) is the most important structure that can sustain the jet of secondary air very long in the flow field, it also lifts secondary air flow off the protected surface what allows mainstream air to enter under it.

Figure-5 shows the vorticity contours on normal plane at x/d = 3.0. The pair of positive and negative vorticity was the counter rotating vortex pair (CRVP), and it promoted the secondary air to separate from the wall surface. The vortex pair of (B) was a twins vortex generated when the mainstream passes through the side and the upper surface of AVG, their rotation was opposite to CRVP. In case 01 at BR = 0.5, CRVP observed by z/d = 0.0 became large. It is because CRVP and vortex pair (B) interacted each other in this region and the vorticity was emphasized. As for case 02, since the location in which the vortex generated from AVG shifted from the center, the CRVP became asymmetrical. In case 03 and case 04, the vortex generated from AVG moved to the location as in Figure-5 (a) (C) because this vortex interacted with CRVP, the secondary air became attached to the wall surface. From case 04 until case 08, there are dispersion and seperation of CRVP which allows to secondary air to mixe very well with mainstream air and investigate high lateraly coverage and maximum value of cooling effectivness along a wall surface. For high BR at 1.0, the high velocity for secondary air will increse CRVP and make it large because the jet of secondary air so high and does not attach the wall surface so, the mainstream air does not effect of secondary air jet.

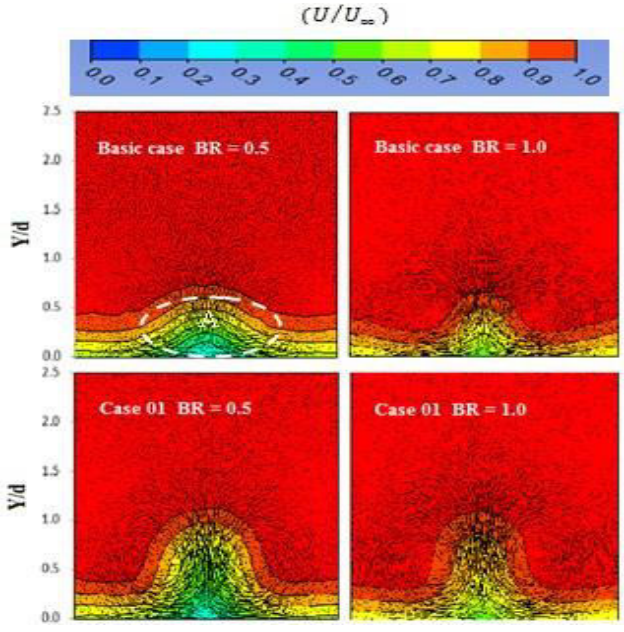

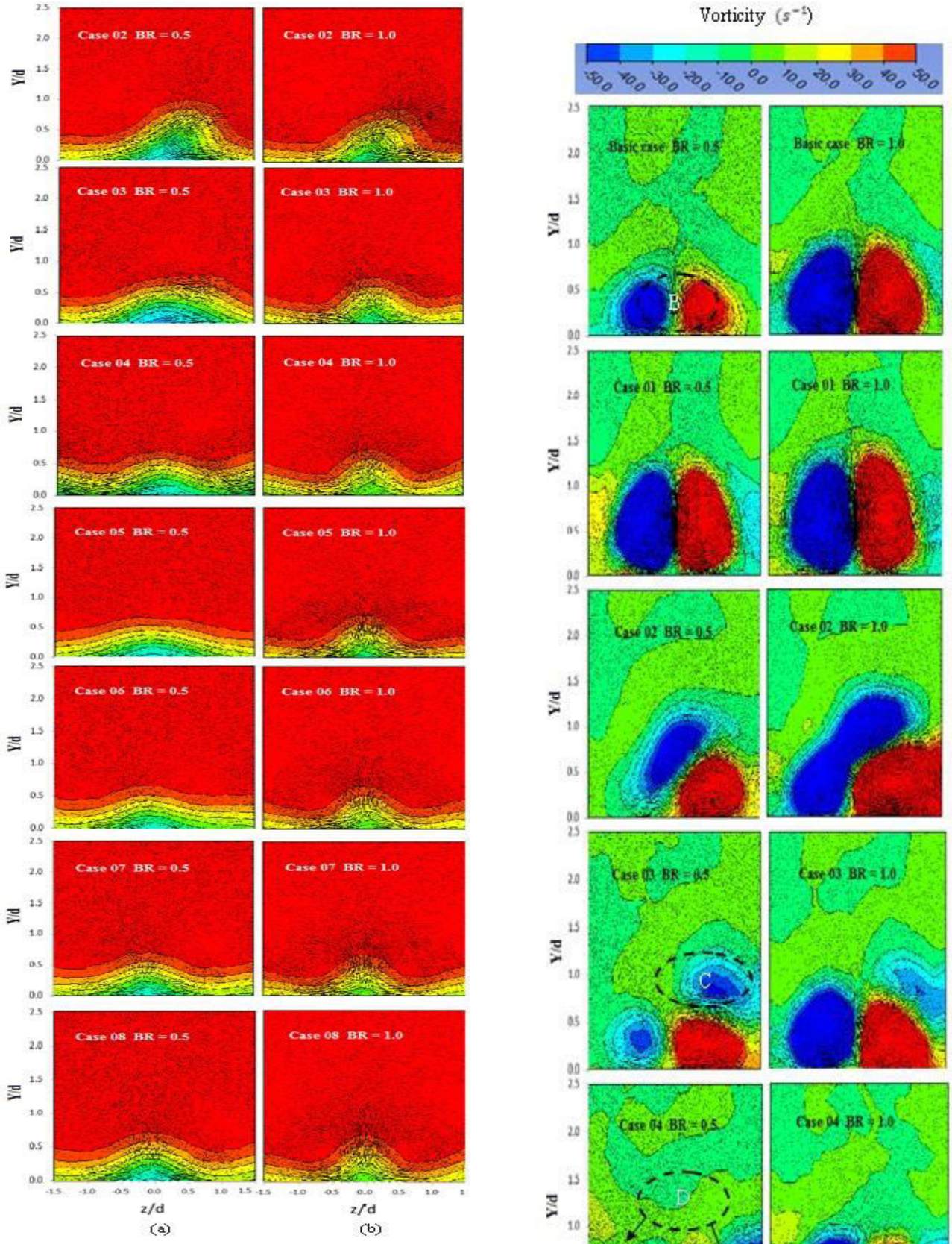

Figure-4. Velocity ratio (U/U_{∞}) in YZ plane at normal plane distance ratio x/d = 03 for all study cases at blowing ratios (a) BR = 0.5 and (b) BR = 1.0.

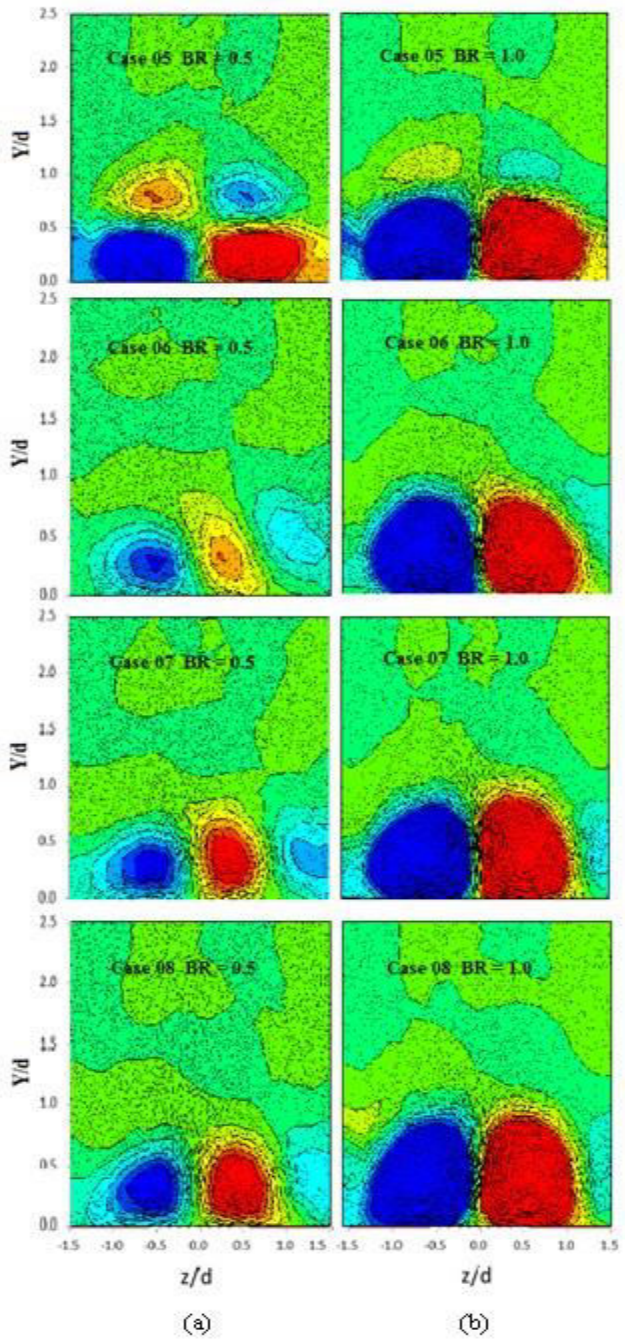

Figure-5. Vorticity in YZ plane at normal plane distance ratio x/d = 03 for all study cases at blowing ratios (a) BR = 0.5 and (b) BR =1.0.

Film cooling effectiveness

Figure-6 (a) shows the distribution of film cooling effectiveness on the wall surface at BR = 0.5 obtained by CFD simulation. In basic case, the the film cooling effectiveness expanded symmetrical in mainstream direction on the center line. In case 01, the film cooling effectiveness did not expand too much in mainstream direction and only the film cooling effectivenss on the center line because the secondary air became high. In case 02, the extension and distribution of film cooling effectiveness improved because of the shifting (AVG) position and the reason of that the mixing between mainstream air and secondary air promoted a little bit. On the other hand, case03 and case 04 had wide film cooling effectiveness distribution in mainstream direction. The film cooling effectiveness distribution was asymmetrical to the center line because the secondary air was bent by the vortex structure generated from AVG. In case 05-case 08 had similar distribution of film cooling effectiveness with that of basic case except case 06 had similar distribution with case 04. The best cases that have long extension in mainstream direction were case 05 and case 07. However, the local film cooling effectiveness in these cases were slightly high and it was shown that mixing of the mainstream and secondary air was promoted in these cases. Figure-6 (b) shows the distribustion of film cooling effectiveness on the wall surface at BR = 1.0. In these conditions, since the velocity in secondary air increased, the film cooling effectiveness became low compared with the BR = 0.5 condition. Generally, the extension and distribution of film cooling effectiveness was less than the cases at BR = 0.5. The best cases that have long extension of film cooling effectiveness were case 03, case 04 and case 06.

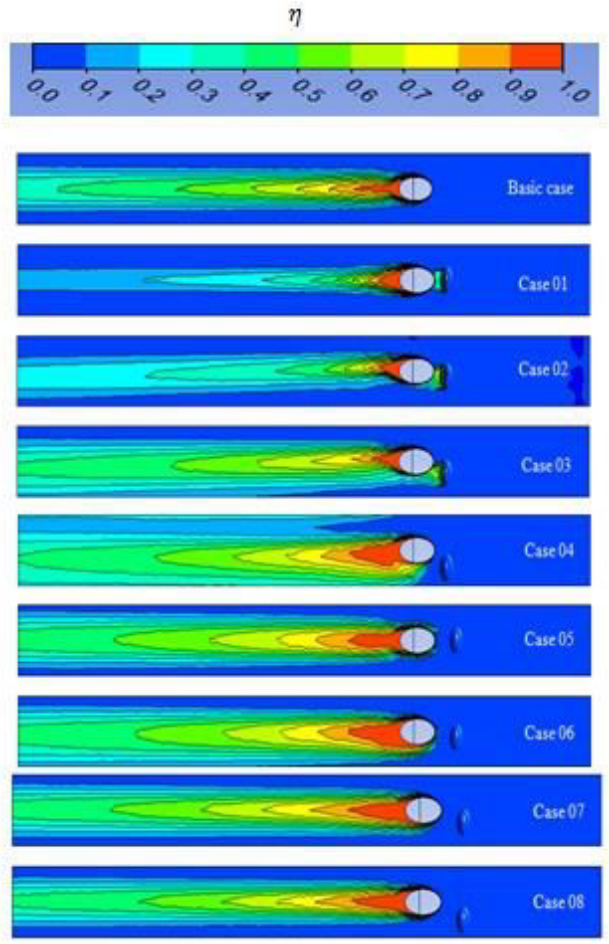

Figure-6. (a). Distribution of film cooling effectiveness on the wall surface at BR = 0.5.

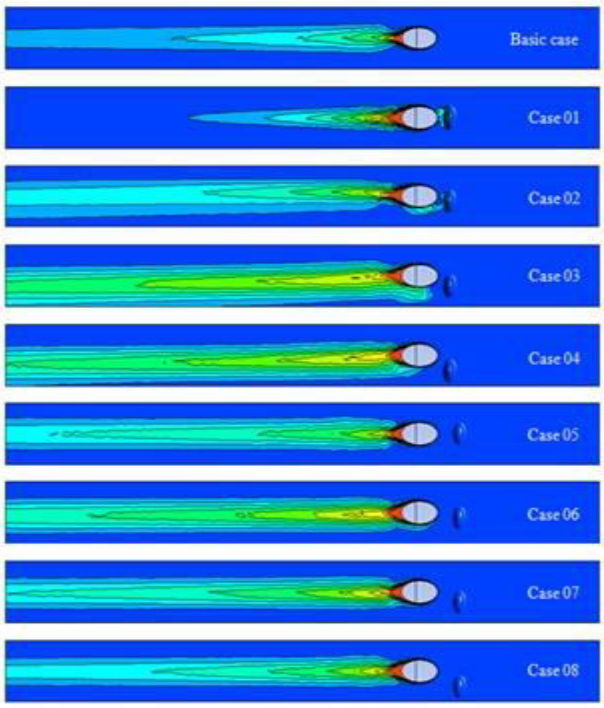

Figure-6. (b). Distribution of film cooling effectiveness on the wall surface at BR = 1.0.

Figure-7 shows the comparison of laterally averaged film cooling effectiveness between all cases of study. As seen in the figure at BR = 0.5, the best case of this comparison is case 04 and case 06, also from figure the averged film cooling effectiveness for basic case was higher than case 01 and case 02 that is because the distribution of film cooling effectiveness was symmetrical on the center line and wide. From case 03, the film cooling effectiveness begian increase slightly to case 04 and then there is little bit decreased of film cooling effectiveness for last four cases. In general, last four cases were better than first four cases except case 04 that is because the interaction between the mainstream and secondary air was promoted and gave symmetrical distribution for film cooling effectiveness on the center line. At BR = 1.0, case 03 was the best case.

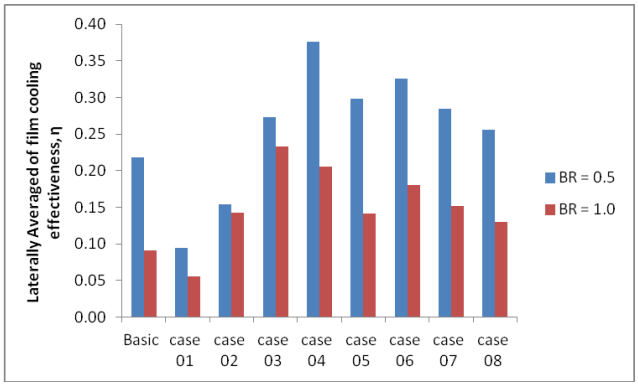

Figure-7. Comparison of laterally averaged film cooling effectiveness between all cases of study at different BR.

Figure-8 shows the comparison of maximum film cooling effectiveness between all cases of study at different BR, as seen in the figure basic case and last four cases were the highest that cause the distribution of film cooling effectiveness was symmetrical and expand on the center line. Case 03 and case 04 were lower than last four cases that because there are little bit shift of film cooling effectiveness distribution on the center line and coverage more area for wall surface.

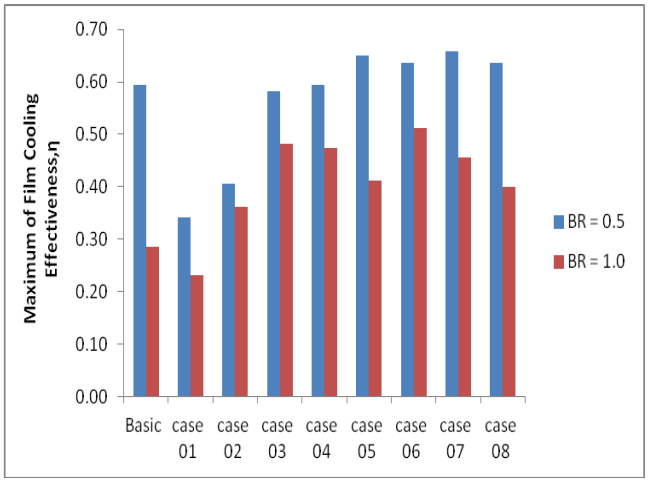

Figure-8. Comparison of Maximum film cooling effectiveness between all cases of study at different BR

VALIDATION OF COMPARISON RESULTS

The validation of current study was based on the result that obtained from journal done by Hirokazu K, *et al.* (2014). Figure-9 shows the spatially averaged film effectiveness for both validation results. The spatially averaged film effectiveness was calculated in the region of x/d = 0-10. It was normalized with the spatially averaged film effectiveness of Basic case at BR = 0.5. The validation is only for 5 cases which are from basic case to case 04 at same BR.

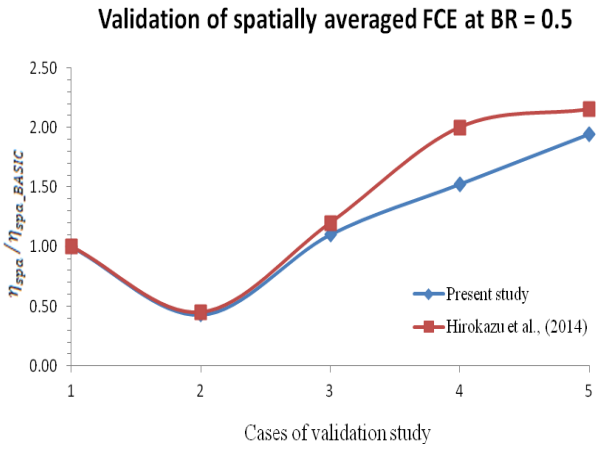

Figure-9. Validation of spatially averaged film effectiveness at BR = 0.5.

From Figure-9, shows a slight different between this present study result and Hirokazu *et al.* (2014) result. The reason of this cause might be that the Hirokazu *et al.* (2014) result was based on experimental result instead of using CFD simulation to obtain the result. The percentage error was 9.15% estimated by using the relative absolute error (RAE) method. So, the slight different of present study result and Hirokazu *et al.* (2014) result was acceptable.

ACKNOWLEDGEMENTS

The authors gratefully acknowledge ministry of higher education, Malaysia for the financial support.

CONCLUSIONS

From obtained results, the changing of (AVG) design improved the distribution of film cooling effectiveness as well as increased the extension of film cooling effectiveness. As well, the analyzed results of cases show that in first design, case 04 had a good coverage on the wall surface. While in second design, all cases had symmetrical distribution better than the cases in first design. The validation of present results have been implemented in order to confirm the validity of present results with (Kawabata *et al.* 2014). Thus, the comparison results showed that the percentage error was 9.15% which estimated by using (RAE) method. From Figure-9, the difference between present study and (Kawabata *et al.* 2014) was slightly and acceptable.

REFERENCES

[1] Azzi, A., and Jubran A.B., "Numerical modelling of film cooling from converging slot-hole," Heat Mass Transf., vol. 43, no. 4, pp. 381–388, Mar. 2006.

[2] Barigozzi, G., Franchini, G., and Perdichizzi, A., 2007, "The Effect of an Upstream Ramp on Cylindrical and Fan-Shaped Hole Film Cooling—Part 2: Adiabatic Effectiveness Results," ASME Paper No. GT2007-27079.

[3] Barigozzi, G., Franchini, G., and Perdichizzi, A., 2007. "The Effect of an Upstream Ramp on Cylindrical and Fan-Shaped Hole Film Cooling—Part 1: Aerodynamic Results," ASME Paper No. GT2007-27077.

[4] C. H. N. Yuen and R. F. Martinez-Botas, "Film cooling characteristics of a single round hole at various streamwise angles in a crossflow: Part I effectiveness," Int. J. Heat Mass Transf., vol. 46, no. 2, pp. 221–235, Jan. 2003.

[5] Christain, S., and Achmed, S., "Effect of Geometry Variations on the Cooling Performance of Fan Shaped Cooling Holes," ASME Turbo Expo, Berlin, 2008. GT2008-51038.

[6] Goldstein, R. J., Eckert, E. G., and Burggraf, R., 1974, "Effects of Hole Geometry and Density on Three Dimensional Film Cooling," Int. J. of Heat and Mass Transfer, 17, pp. 595–606.

[7] H. Kawabata, K.-I. Funazaki, R. Nakata, and D. Takahashi, "Experimental and Numerical Investigations of Effects of Flow Control Devices upon Flat-Plate Film Cooling Performance." J. Turbomach., vol. 136, no. 6, pp. 0610211–6102111, Jun. 2014.

[8] Haven, B. A., Yamagata, D. K., Kurosaka, M., Yamawaki, S., and Maya, T., 1997, "Anti-Kidney Pair of Vortices in Shaped Holes and Their Influence on Film Cooling Effectiveness," ASME Paper No. 97-GT-45.

[9] Heneka, C., Bauer, H.J., Heselhaus, A., Crawford, M., and Schwlz, A "Film Cooling Performance of Sharp Edged Diffuser Holes With Lateral Inclination," ASME, vol. 134(4), 04, no. 4, p. 8 pages, 2012.

[10] Na, S., and Shih, T., 2007. "Increasing Adiabatic Film-Cooling Effectiveness by Using an Upstream Ramp," ASME J. Heat Transfer, 129, pp. 464–471